Partial and complete periodic synchronization in coupled discontinuous map lattices*

Yang Ke-Li(杨科利)[a)b)], Chen Hui-Yun(陈会云)[a)], Du Wei-Wei(杜伟伟)[a)], Jin Tao(金 涛)[a)], and Qu Shi-Xian(屈世显)[a)†]

[a)] *Institute of Theoretical and Computational Physics, School of Physics and Information Technology, Shaanxi Normal University, Xi'an* 710062, *China*

[b)] *Nonlinear Research Institute, Baoji University of Arts and Sciences, Baoji* 721016, *China*

(Received 15 December 2013; revised manuscript received 25 February 2014; published online 15 May 2014)

The partial and complete periodic synchronization in coupled discontinuous map lattices consisting of both discontinuous and non-invertible maps are discussed. We classify three typical types of periodic synchronization states, which give rise to different spatiotemporal patterns including static partial periodic synchronization, dynamically periodic synchronization, and complete periodic synchronization patterns. A special prelude dynamics of partial and complete periodic synchronization motion, which is shown by five separated concave curves in the time series plots of the order parameters, is observed. The detailed analysis shows that the special prelude dynamics is induced by the competition between two synchronized clusters, and the analytical expression for the corresponding order parameter is obtained.

Keywords: discontinuous map, coupled map lattices, periodic synchronization, prelude dynamics

PACS: 05.45.Ra, 05.45.–a **DOI:** 10.1088/1674-1056/23/7/070508

1. Introduction

Since the pioneering work of Hungens, synchronous behavior has been widely observed in a large range of phenomena that span from biological systems that include animal grouping,[1] fireflies blinking,[2] animal gaits,[3] heart stimulation,[4] epidemiology[5] and neural activity,[6] to secure communications,[7] chemistry,[8] meteorology,[9] and optoelectronics.[10] Recently, there have been many analysis methods appearing in the vast technical literature on synchronization, including the master stability function (MSF),[11–13] eigenvalue analysis[14] and more advanced techniques, allowing one to solve synchronization problem in the network of any set of coupling weights, connections, and the number of the coupled oscillators. However, the great majority of those research efforts have focused on dynamical systems that consist of smooth dynamical models.[15–18] In fact, there are many practical systems that show discontinuous dynamical properties, such as nerve cells,[19] electronic circuits,[20] relaxation oscillators, and impact oscillators.[21–25]

Here we study the synchronized patterns on the coupled map lattices (CMLs) whose individual dynamics is both discontinuous and non-invertible. One of the authors and his cooperators have conducted intensive investigation on those kinds of individual dynamical systems, and found new types of characteristic dynamics compared with those in systems that are smooth everywhere, which include type-V intermittencies,[23] hole-induced crises,[25] multiple Devil's staircases,[26] coexistence of attractors,[27,28] and so on. Recently, coupled discontinuous (non-differentiable) dynamical systems have received much interest from researchers.[24,29–33] For example, Zou[33] studied high-dimensional discontinuous dynamical systems, and revealed a mechanism for the formation of stable chaos. Our recent study on globally coupled discontinuous map lattices systems[34] shows that there are rich collective dynamic behaviors due to the interplay between the discontinuity and the non-invertibility in the isolate map. However, periodic synchronization in coupled discontinuous systems has been studied much less.

In the previous studies, the periodic synchronized state is a frozen random pattern, the dynamical behaviors on both sides of the kinks or anti-kinks do not correlate with each other, and thus the space is divided into separate domains with random sizes by the fixed interfaces that do not move with time.[35] In this paper, we focus on the study of partial and complete periodic synchronized patterns in CMLs. The constituent of the CMLs employed in this work is both a discontinuous and a non-invertible map, which is a simplification of the relaxation oscillators described in the previous work.[24] Three typical types of periodic synchronization states are obtained: static partial periodic synchronization, dynamically periodic synchronization, and complete periodic synchronization patterns. The dynamically periodic synchronization is a new phenomenon, in which the space is divided into two clusters in the coupled discontinuous system, compared with the previous studies,[36,37] the interfaces of the clusters are no longer fixed but moving in opposite directions, and the size of cluster changes with time. The transient state dynamics of the complete periodic synchronization also displays a similar phe-

*Project supported by the National Natural Science Foundation of China (Grant No. 10875076) and the Natural Science Foundation of Shaanxi Province, China (Grant No. SJ08A23).

†Corresponding author. E-mail: sxqu@snnu.edu.cn

© 2014 Chinese Physical Society and IOP Publishing Ltd

nomenon.

Because of the important position of discontinuous features in the study of neurons firing,[38,39] our study may be enlightening for the further understanding of some aspects of the dynamics of the brain networks. Moreover, due to the discontinuous map being a simplied model for relaxation oscillator circuits, the dynamically periodic can also be a potential application in chaos communication; we have already done some research there, and the detailed results will be coming soon.

2. Model

The evolution equations for the coupled discontinuous map lattices in the current work can be expressed as

$$x_{n+1}(i) = (1-\varepsilon)f(x_n(i)) + \frac{\varepsilon}{2}[f(x_n(i+1)) + f(x_n(i-1))], \quad (1)$$

where $x_n(i)$ is the dynamical variable, $i = 1,2,3,\ldots,N$ denotes the discrete spatial sites, n is the temporal step, and ε ($0 \le \varepsilon \le 1$) is the coupling strength. The periodic boundary condition $x_n(i) = x_n(i+N)$ is assumed. The $f(x)$ is a piecewise linear mapping function with both discontinuous and non-invertible characteristics,[25] which reads

$$x_n = f_m(x_n) = k_m x_n + b_m \bmod 1, \quad (2)$$

with $m = 1,2,3,4$, and

$$\begin{aligned}
k_1 &= \frac{y_a - y_a - \mu}{x_b - x_a}, \quad b_1 = y_a, && x \in [x_a, x_b];\\
k_2 &= \frac{y_c - y_a + \mu}{x_g - x_b}, \quad b_2 = y_A - \mu - k_2 x_b, && x \in [x_b, x_g];\\
k_3 &= \text{constant}, \quad b_3 = \text{constant}, && x \in [x_g, x_f];\\
k_4 &= \text{constant}, \quad b_4 = \text{constant}, && x \in [x_f, x_d],
\end{aligned}$$

where μ is the control parameter. The other parameters are selected as $x_a = 0$, $y_a = 0.203921$, $x_b = 0.107663$, $x_g = 0.350000$, $y_c = 0.460000$, $x_f = 0.497121$, $x_d = 1$, $y_d = y_A$, $k_3 = 3.07055$, $b_3 = -0.530165$, $k_4 = 0.405507$, and $b_4 = -0.201586$. It has been shown that this map can exhibit rich dynamical behaviors when the control parameter μ increases from 0.025 to 0.065.[24] In this work, the system size is set to $N = 100$, and the control parameter is $\mu = 0.026921$ where the period-5 dynamics appears.

3. Partial and complete periodic synchronization

The initial values of the dynamical variables in the numerical simulations are chosen randomly from the range [0,1]. The order parameter[40] and the largest Lyapunov exponent $\lambda_{\max}$ are employed to monitor the spatiotemporal dynamics of the system. The order parameter is defined in the following way:

$$z_n = R_n \exp(\mathrm{i}\varphi_n) = \frac{1}{N}\sum_{j=1}^{N} \exp(2\pi \mathrm{i} x_n^{(j)}), \quad (3)$$

where R_n and φ_n are the magnitude and phase of z_n at time n, respectively. The order parameter tends to unity when the system approaches the synchronized state where the dynamical variables on the lattices reach the same amplitudes. The time-average of the order parameters is often used, which is defined by

$$\langle R \rangle = \lim_{T\to\infty} \frac{1}{T} \sum_{n=m}^{T} R_n, \quad (4)$$

where m is the number of transients that should be discarded. Figure 1 shows the coupling-strength dependence of the time-averaged order parameter $\langle R \rangle$ and the largest Lyapunov exponent $\lambda_{\max}$, where 1×10^6 transients were dropped and 5×10^4 iterations were used for the time average.

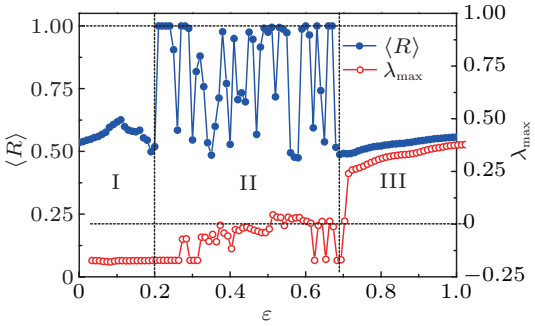


Fig. 1. (color online) The time-average order parameters and the largest Lyapunov exponents, where the dots denote the order parameters, and the circles represent the largest Lyapunov exponents for $\mu = 0.026921$. The size of the system is set to $N = 100$ and the random initial values are chosen in simulation.

One can see that, there are basically three regions in the ε axis: region I is confined by $0 < \varepsilon < 0.2$, region II is confined by $0.21 < \varepsilon < 0.67$ and region III by $0.67 \le \varepsilon < 1$. In region I, the order parameters are less than 1 and the largest Lyapunov exponents have a negative value, which reveals the periodic motion of the system and that it is not fully synchronous. The order parameters are less than 1 and the largest Lyapunov exponents are greater than zero in region III (see Fig. 1), which indicates that the system is in the nonsynchronized chaotic state. The spatial-temporal dynamics behaviors in the previous regions are very trivial, which are not topics of the current work. While in region II, the order parameter and the largest Lyapunov exponent fluctuate fiercely. There are some points in the ε axis where the average order parameter reaches unity and the largest Lyapunov exponent has a negative value, so there are partial and complete periodic synchronized states in this region. If the order parameter is less than 1 and the largest Lyapunov exponent has a negative value, the coupled system displays a dynamical periodic synchronized pattern. More information on the partial and complete periodic synchronization can also be visualized by using a space–time plot (see Fig. 2).

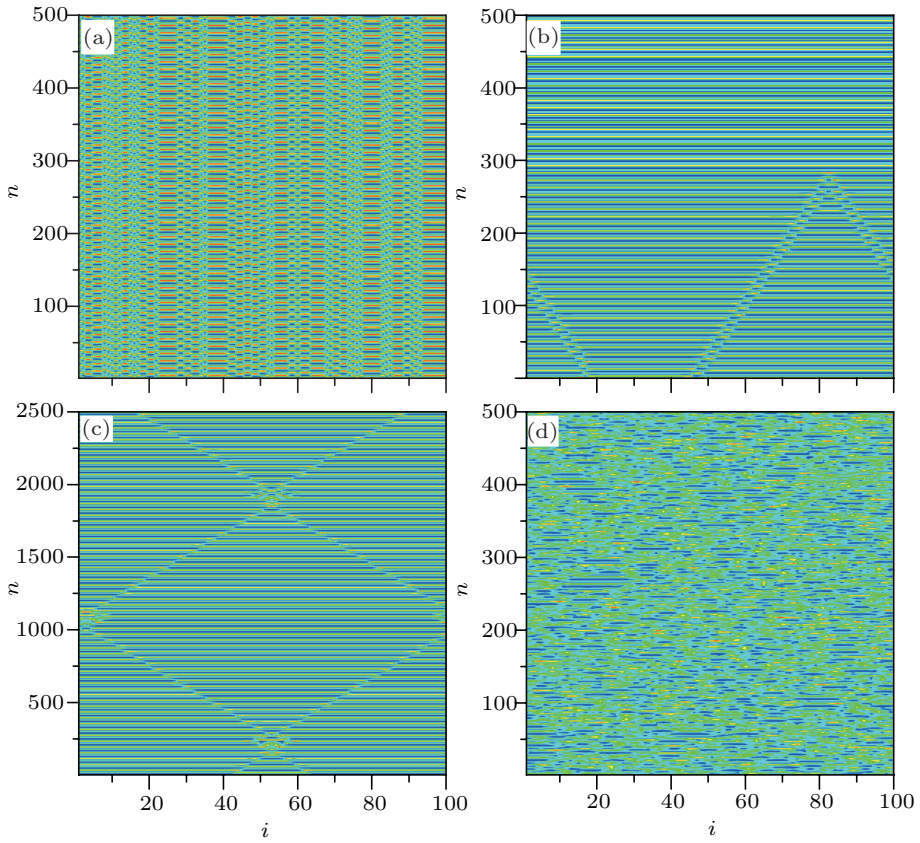


Fig. 2. (color online) The space–time plots for different coupling strengths ε: (a) $\varepsilon = 0.1$, (b) $\varepsilon = 0.21$, (c) $\varepsilon = 0.31$, (d) $\varepsilon = 0.7$. The size of the system is set to $N = 100$ and with the random initial values chosen in simulation, and 1×10^6 transients were discarded.

In Fig. 2(a), the partial periodic synchronized patterns with the temporal period equal to that of the individual map are shown in the space–time plots. The dynamical behaviors on both sides of the kinks or anti-kinks do not correlate with each other, and thus the space is divided into separate domains with random size by the fixed interfaces that do not move with time. The nodes in each domain synchronized to the same period-5 orbit of the isolated map, while the dynamics in different domain slides in different steps of the same period-5 cycle. Therefore, the frozen random pattern is observed, which is similar to that observed in the conventional CMLs of the smooth maps. We have to emphasize that the distribution of the patterns depends on the choice of the initial condition. Here, the randomly distributed pattern of the attractors is due to the random initial condition. The space–time plots in Figs. 2(b) and 2(c) exhibit different patterns against that in Fig. 2(a). In those cases, the space is divided into two clusters and the interfaces are no longer fixed but moving in opposite directions. Synchronization to the period-5 orbit of the isolated map is observed in each cluster, but the trajectory in one domain is one step ahead of or behind that of the other one. In Fig. 2(b), one may find that one of the domains expands but the other shrinks. The trajectories of nodes in the contracting cluster and the expanding cluster synchronize to two adjacent fixed points of the period-5 cycle, respectively. The fixed point for the former cluster is one step ahead of that for the latter. When the two boundaries collide with each other, the expanding cluster occupies nearly all the space and then the system reaches the complete synchronization afterward. A dynamical synchronized pattern is shown in Fig. 2(c), in which, one also observes a pair of clusters that exhibit similar behaviors to the previous case, i.e., one of them expands but the other contracts. We call it a long time process. When there is only one node left in the contracting cluster, a short time process begins, in which this contracting cluster no longer shrinks but expands. When it expands to some extent, it goes inversely till the two boundaries re-meet. After this instant, the system evolves along the inverse direction of the long process mentioned previously. When the boundaries collide again, the same long time process starts. The system will repeat the two processes again and again till infinity. This is a very interesting dynamics behavior, which will be discussed elsewhere in another long paper. If the coupling strength ε exceeds 0.67, the partial and complete periodic synchronization is impossible to achieve and the coupled system is in the chaotic state, as shown in Fig. 2(d), which is a very trivial behavior.

The dynamical behaviors described above can also be monitored through the corresponding average order parameters, as shown in Fig. 3. One may observe in Fig. 3(a) that the order parameter falls in five separated horizontal lines, which indicates that the order parameter varies with time in a period-5 cycle. It can be easily understood by considering the frozen

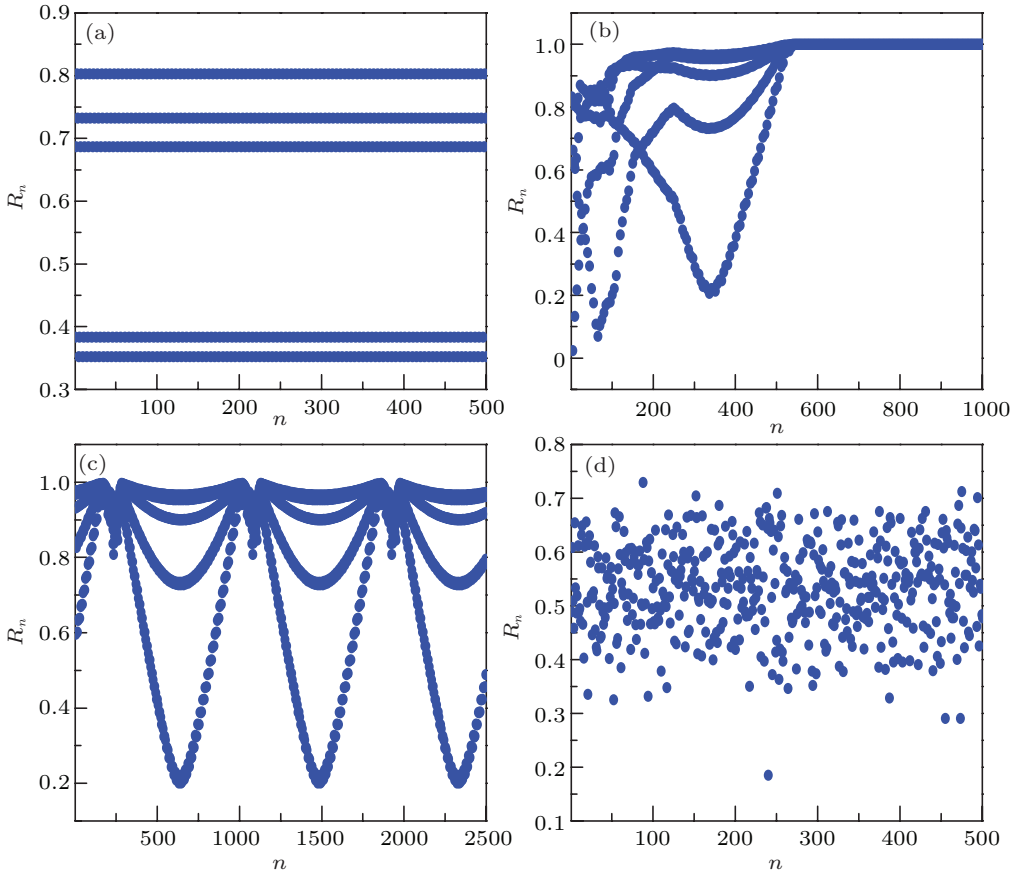


Fig. 3. (color online) Time series of the order parameter for different coupling strengths ε: (a) $\varepsilon = 0.1$, (b) $\varepsilon = 0.21$, (c) $\varepsilon = 0.31$, (d) $\varepsilon = 0.7$. The other parameters are the same as those in Fig. 2.

random pattern displayed by Fig. 2(a). The dynamical states of the nodes in each domain at any time steps are in the same trajectory of the same period-5 orbit, and the only possible change is that the dynamics in different domains may be in different steps (or different fixed-points) of the same period-5 orbit. Thus, the synchronization occurs only inside the same domain but not necessarily among different domains, which results in partial synchronization. Therefore, the system has different order parameters at different time steps, and the order parameter changes with time in the same period as that of the system dynamics. While in Figs. 3(b) and 3(c), there are only two domains and two boundaries that are moving oppositely with respect to time. The synchronized states in two domains fall in the same period-5 cycle of the isolated map, but the trajectory for one domain is one step ahead of or behind that for the other one (or in adjacent fixed-points of the same period-5 orbit). Since one of the domains expands and the other shrinks, one observes that the order parameters in Fig. 3(b) before the complete synchronization and Fig. 3(c) in all time fall in five separate concave curves instead of the straight ones in Fig. 3(a). Figure 3(d) represents a very trivial result that the system is in the non-synchronized chaotic state. Amongst the four plots in Fig. 3, we are only interested in the situation appearing in Fig. 3(b) in which a peculiar prelude dynamics emerges before the system reaches the complete synchronization. We will discuss this prelude dynamics in the following section.

4. The peculiar prelude dynamics to periodic synchronization

In order to understand the special behavior of the order parameters in the above section, the space–amplitude diagrams near temporal points A, B, and C corresponding to the third curve from the bottom of Fig. 3(b), are plotted in Fig. 4 for every five time steps, respectively. Clearly, the spatial sites are catalogued into a pair of clusters, i.e., the lower one and the upper one, and only very few sites are on the boundaries between the pair of clusters. The dynamical variables of the nodes in each cluster synchronize to the same period-5 orbit of the isolated map, but the trajectory of the lower cluster is one step ahead of that of the upper one. If we arrange the trajectories of the period-5 cycle according to an ascending order and assume that the trajectory of the lower cluster is at an arbitrary n-th step of a time sequence, then the trajectory of the upper cluster is the same as the trajectory at the $(n+1)$-th step. From Fig. 4(a) to Fig. 4(d), the boundaries of the two clusters move in opposite directions, which results in the shrinking of the lower cluster and the expanding of the upper one. For convenience, we call the lower cluster the contracting cluster and the upper one the expanding cluster. Thus the trajectory of the contracting cluster of the pair is at the n-th time-step, and that of the expanding clusters of the pair is the same as the

trajectory at the $(n+1)$-th time-step. In Fig. 4(e), the lower cluster vanishes, the upper cluster occupies nearly all of the nodes in the system, and leaves only the boundary sites non-synchronized. Very soon after this instant, the boundary sites also synchronize to the upper cluster and the system reaches the complete period synchronization, as shown in Fig. 4(f).

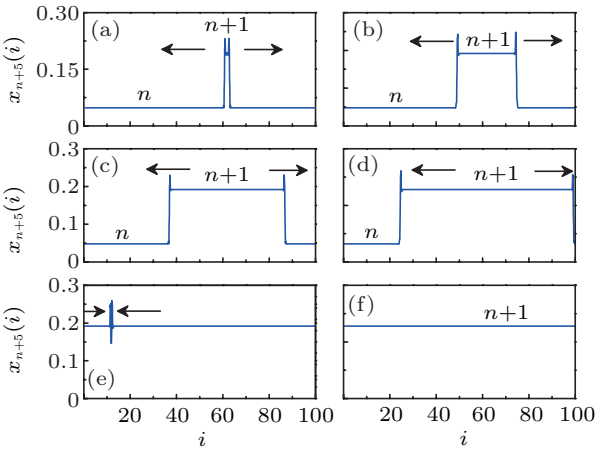


Fig. 4. (color online) Space-amplitude plots at temporal points from A to C and corresponding to the third curve from the bottom of Fig. 3(b). The spatial sites are catalogued into a pair of clusters: a contracting and expanding cluster, the contracting cluster of the pair is at the n-th time-step, the expanding clusters of the pair is the same as the trajectory at the $(n+1)$-th time-step. (a)–(d) The lower cluster shrinks and the upper cluster expands at different moments. (e) In the collision point, the lower cluster vanishes and the upper cluster occupies nearly all of the nodes in the system. (f) All of the nodes synchronize to the upper cluster, and the system reaches the complete period synchronization.

Similar behaviors are also observed in the situations corresponding to the other four curves in Fig. 3(b). For comparison, we have drawn in Fig. 5 the space–amplitude plots within a period-5 cycle somewhere between points A and C according to an ascending order. The trajectories of the contracting clusters are at the n-th, $(n+1)$-th, $(n+2)$-th, $(n+3)$-th, and $(n+4)$-th time-steps, which are respectively the fixed points of the period-5 orbit of the isolated map. While the trajectories of the corresponding expanding clusters are the same as those at the $(n+1)$-th, $(n+2)$-th, $(n+3)$-th, $(n+4)$-th, and $(n+5)$-th time-steps. Clearly, one may find that the five plots show the same pattern and the size of the pair of contracting and expanding clusters remains unchanged in one period. Hence, the size of the clusters varies for every five-steps. In order to determine the variation of the size of the cluster pair, we employ the direction phase proposed by Hu and Liu,[41] which reads

$$P_n(j) = \begin{cases} 1, & \text{if } x_n(j)/x_{n+1}(j) > 1, \\ 0, & \text{otherwise}, \end{cases} \tag{5}$$

where j denotes the nodes, and $x_n(j)$ is the dynamical variable for the j-th node at time step n. Shown in Fig. 5, the expanding and the contracting clusters in the first three time-steps have the same phase order, while those in the last two time-steps have the opposite phase order. Therefore, we can distinguish the expanding and the contracting clusters and then calculate

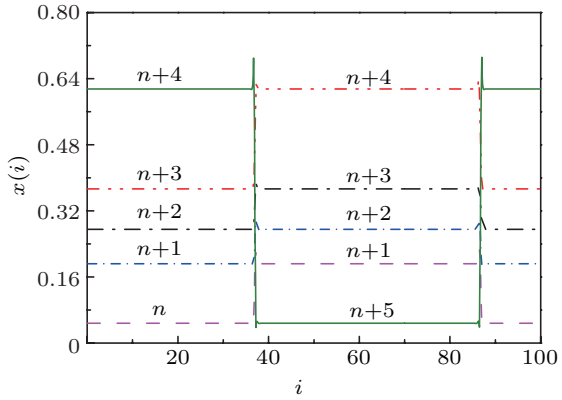


Fig. 5. (color online) Space-amplitude plots for the period-5 cycle near point B in Fig. 3, and arrange the trajectories of the period-5 according to the ascending order, the trajectories of the contracting clusters are at the n-th, $(n+1)$-th, $(n+2)$-th, $(n+3)$-th, and $(n+4)$-th time-steps, the trajectories of the corresponding expanding clusters are the same as those at the $(n+1)$-th, $(n+2)$-th, $(n+3)$-th, $(n+4)$-th, and $(n+5)$-th time-steps.

the size of the clusters in terms of the phase order by tracing the iteration of the trajectories of the dynamics on the nodes when those in the contracting cluster reach the fourth or fifth fixed point of the isolated map. For the latter case, one may see that $P_n(j) = 0$ for each node in the contracting cluster, while $P_n(j) = 1$ for each node in the corresponding expanding cluster. Then, the size of the contracting cluster can be represented by the number fraction $\rho_n^{(0)} = (1/N)\sum_{j=1}^{N}(P_n(j) = 0)$, and the size of the expanding one by $\rho_n^{(1)} = (1/N)\sum_{j=1}^{N}(P_n(j) = 1)$. As discussed previously, almost all of the lattices belong to the pair of clusters and only a tiny number of the sites are on the boundaries. Hence, equation (3) can be rewritten as

$$z_n \approx \rho_n^{(0)} \exp(2\pi \mathrm{i} x_n^*) + \rho_n^{(1)} \exp(2\pi \mathrm{i} x_{n+1}^*), \tag{6}$$

where x_n^* and x_{n+1}^* are two adjacent fixed points of the five fixed points of the single map defined in Eq. (2). Simple derivation gives the analytical expression of the order parameter, i.e.,

$$\begin{aligned} R_n = & \{(\rho_n^{(1)})^2 + (\rho_n^{(0)})^2 \\ & + 2\rho_n^{(1)}\rho_n^{(0)} \cos[2\pi(x_{(n+1)}^* - x_{(n)}^*)]\}^{1/2}. \end{aligned} \tag{7}$$

Shown in Fig. 6 are the analytical results of the order parameter calculated by Eq. (7) and its numerical counterpart. The circles denote the numerical result, and the lines represent the analytical one. Obviously, the analytical and numerical results agree with each other very well. To this end, one may conclude that the specular prelude dynamics has been completely understood. We have to point out that the analytical method can also be used to analyze the dynamically synchronous patterns, which will be discussed elsewhere.

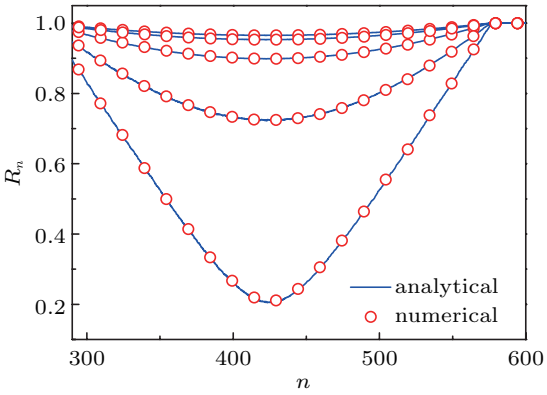


Fig. 6. (color online) The analytical result of the order parameter calculated by Eq. (7) and its numerical counterpart. The red circles donate the numerical result, and the blue line represents the analytical one.

5. Conclusion

In summary, we have studied the periodic synchronized patterns in a coupled discontinuous and non-invertibility map lattices with local coupling, and found three periodic periodic synchronized patterns: the static partial periodic synchronized pattern, the dynamical periodic synchronized pattern, and complete periodic synchronized patterns. The results show that spatial sites of the coupled system are catalogued into a few clusters, only very few sites are on the boundaries between the pair of clusters, and the interplay between synchronization clusters is responsible for these characteristic patterns. Moreover, a peculiar prelude dynamics, which is shown by five separated concave curves in the time series plots of order parameters, is identified. The analysis shows that one of the two synchronized clusters contracts and the other expands, which result in the peculiar prelude dynamics. Nevertheless, an analytical expression of the order parameter of the peculiar prelude dynamics is given. The analytical result is found to be in good agreement with the numerical one.

In the present work, the periodic synchronized patterns synchronization in the next nearest neighbor coupling regular network is found. The obtained result depends on the network characteristics. In future works, more performance requirements for the periodic synchronized patterns of a coupled discontinuous system will be considered in various topological structures.

References

[1] Sumpter D J T 2009 *Collective Animal Behavior* (Princeton: Princeton University Press)
[2] Buck J and Buck E 1976 *Sci. Am.* **234** 74
[3] Buono P L and Golubitsky M 2001 *J. Math. Biol.* **42** 291
[4] Guevara M R, Shrier A and Glass L 1988 *Am. J. Physiol.* **254** H1
[5] He D and Stone L 2003 *Proc. R. Soc. London Ser. B* **270** 1519
[6] Womelsdorf T and Fries P 2007 *Curr. Opin. Neurobiol.* **17** 154
[7] Cuomo K M, Oppenheim A V and Strogatz S H 1993 *IEEE Trans. Circ. Syst. II* **40** 626
[8] Kuramoto Y 1984 *Chemical Oscillations, Waves and Turbulence* (Courier Dover Publications)
[9] Duane G S, Webster P J and Weiss J B 1999 *J. Atmos. Sci.* **56** 4183
[10] Yanchuk S, Stefanski A, Kapitaniak T and Wojewoda J 2006 *Phys. Rev. E* **73** 016209
[11] Pecora L M and Carroll T L 1998 *Phys. Rev. Lett.* **80** 2109
[12] Huang L, Chen Q, Lai Y C and Pecora L M 2009 *Phys. Rev. E* **80** 036204
[13] Huang L, Lai Y C, Park K, Wang X G, Lai C H and Gatenby R 2007 *Frontiers of Physics in China* **2** 446
[14] Yang J, Hu G and Xiao J 1998 *Phys. Rev. Lett.* **80** 496
[15] Fu C B, Zhang H, Zhan M and Wang X G 2012 *Phys. Rev. E* **85** 066208
[16] Fu C B, Deng Z G, Huang L and Wang X G 2013 *Phys. Rev. E* **87** 032909
[17] Liu Z H, Zhou J and Munakata T 2009 *Euro. Phys. Lett.* **87** 50002
[18] Liu Z H and Zhou J 2008 *Phys. Rev. E* **77** 056213
[19] Glass L and Belair J 1986 *Lect. Notes. Biomath.* **66** 232
[20] Fang J Q, Luo X S, Wang B H and Zhao Y B 2005 *Acta Phys. Sin.* **54** 5022 (in Chinese)
[21] He D R, Wang B H, Bauer M, Habip S, Krueger U, Martienssen W and Christiansen B 1994 *Physica D* **79** 335
[22] Dai J, Chu X S and He D R 2006 *Acta Phys. Sin.* **55** 3979 (in Chinese)
[23] He D R, Bauer M, Habip S, Krueger U, Martienssen W, Christiansen B and Wang B H 1992 *Phys. Lett. A* **171** 61
[24] Qu S X, Lu Y Z, Zhang L and He D R 2008 *Chin. Phys. B* **17** 4418
[25] Qu S X, Christiansen B and He D R 1995 *Phys. Lett. A* **201** 61
[26] Qu S X, Wu S G and He D R 1998 *Phys. Rev. E* **57** 402
[27] He D R, Ding E J, Bauer M, Habip S, Krueger U, Martienssen W and Christiansen B 1994 *Euro. Phys. Lett.* **26** 165
[28] Wang C J, Yang K L and Qu S X 2013 *Chin. Phys. B* **22** 030502
[29] Pereira R F, Viana R L, Lopes S R, Verg'es M C and de Pinto S S E 2011 *Phys. Rev. E* **83** 037201
[30] Akaishi A and Shudo A 2009 *Phys. Rev. E* **80** 066211
[31] Miyaguchi T and Aizawa Y 2007 *Phys. Rev. E* **75** 066201
[32] dos Santos A M, Viana R L, Lopes S R, de Pinto S E S and Batista A M 2006 *Physica A* **367** 145
[33] Zou H L, Guan S G and Lai C H 2009 *Phys. Rev. E* **80** 046214
[34] Tan H F, Jin T and Qu S X 2012 *Acta Phys. Sin.* **61** 040507 (in Chinese)
[35] Kaneko K 1989 *Physica D* **34** 1
[36] Qu Z L, Hu G, Ma B and Tian G 1994 *Phys. Rev. E* **50** 163
[37] Willeboordse F H 1993 *Phys. Lett. A* **183** 187
[38] Ibarz B, Casado J M and Sanjuan M A F 2011 *Phys. Rep.* **501** 1
[39] Girardi-Schappo M, Tragtenberg M H R and Kinouchi O 2013 *J. Neurosci. Meth.* **220** 116
[40] Kuramoto Y and Nishikawa I 1987 *J. Stat. Phys.* **49** 1
[41] Hu B and Liu Z H 2000 *Phys. Rev. E* **62** 2114